Elucidating the chemical structure of native 1-deoxysphingosine[s]

Regula Steiner,[1],* Essa M. Saied,[1],[†],[§] Alaa Othman,[2],* Christoph Arenz,[†]
Alan T. Maccarone,** Berwyck L. J. Poad,[††] Stephen J. Blanksby,[††] Arnold von Eckardstein,*
and Thorsten Hornemann[3],*

Institute of Clinical Chemistry,* University and University Hospital of Zurich, CH-8091 Zurich, Switzerland;
Institute for Chemistry,[†] Humboldt Universität zu Berlin, 12489 Berlin, Germany; Chemistry Department,
Faculty of Science, Suez Canal University, Ismailia, Egypt; Mass Spectrometry User Resource and
Research Facility,** School of Chemistry, University of Wollongong, Wollongong, NSW 2522, Australia;
and Central Analytical Research Facility,[††] Institute for Future Environments, Queensland University of
Technology, Brisbane, QLD 4001, Australia

Abstract The 1-deoxysphingolipids (1-deoxySLs) are formed by an alternate substrate usage of the enzyme, serine-palmitoyltransferase, and are devoid of the C1-OH-group present in canonical sphingolipids. Pathologically elevated 1-deoxySL levels are associated with the rare inherited neuropathy, HSAN1, and diabetes type 2 and might contribute to β cell failure and the diabetic sensory neuropathy. In analogy to canonical sphingolipids, it was assumed that 1-deoxySLs also bear a (4E) double bond, which is normally introduced by sphingolipid delta(4)-desaturase 1. This, however, was never confirmed. We therefore supplemented HEK293 cells with isotope-labeled D_3-1-deoxysphinganine and compared the downstream formed D_3-1-deoxysphingosine (1-deoxySO) to a commercial synthetic SPH m18:1(4E)(3OH) standard. Both compounds showed the same m/z, but differed in their RPLC retention time and atmospheric pressure chemical ionization in-source fragmentation, suggesting that the two compounds are structural isomers. Using dimethyl disulfide derivatization followed by MS^2 as well as differential-mobility spectrometry combined with ozone-induced dissociation MS, we identified the carbon-carbon double bond in native 1-deoxySO to be located at the (Δ14) position. Comparing the chromatographic behavior of native 1-deoxySO to chemically synthesized SPH m18:1(14Z) and (14E) stereoisomers assigned the native compound to be SPH m18:1(14Z).[jlr] This indicates that 1-deoxySLs are metabolized differently than canonical sphingolipids.—Steiner, R., E. M. Saied, A. Othman, C. Arenz, A. T. Maccarone, B. L. J. Poad, S. J. Blanksby, A. von Eckardstein, and T. Hornemann. **Elucidating**

Sphingolipids are typically formed by the condensation of serine and palmitoyl-CoA, a reaction catalyzed by the serine-palmitoyltransferase (SPT) enzyme. Besides these canonical substrates, SPT can use other acyl-CoAs, but also alanine or glycine, as substrates, which then form a category of atypical 1-deoxysphingolipids (1-deoxySLs) that lack the C1-OH group of canonical sphingolipids (1, 2).

Several missense mutations in SPT, which are associated with the rare inherited neuropathy, HSAN1, induce a permanent shift in the substrate specificity of the enzyme resulting in increased 1-deoxySL formation. HSAN1 is a rare autosomal and dominantly inherited axonopathy and is clinically characterized by a progressive loss of pain and

temperature sensation, often accompanied by neuropathic pain attacks and skin ulcers (3). The 1-deoxySLs are toxic to primary sensory neurons in culture and lead to neurite retraction and the disruption of the neuronal cytoskeleton structure in a dose-dependent manner (3, 4). They also interfere with the survival and insulin secretory capacity of pancreatic β cells and 1-deoxySL plasma levels have been found to be prospective biomarkers for the risk to develop diabetes type 2 (5–7).

The 1-deoxysphinganine (1-deoxySA), which is formed by SPT, can be converted to 1-deoxyceramides, but not to complex sphingolipids, because of the missing 1-OH group. During catabolism, 1-deoxyceramide is degraded by ceramidase to form 1-deoxysphingosine (1-deoxySO), but is not phosphorylated to form the catabolic intermediate, sphingosine-1-phosphate (S1P). This prevents its cleavage to hexadecenal by S1P-lyase, meaning that 1-deoxySLs cannot be degraded by the canonical catabolic pathway (2). Apart from that, it was assumed that 1-deoxySA is metabolized by the same set of enzymes as canonical sphingoid bases and that 1-deoxySO, like sphingosine, bears a (4E) double bond that is introduced by the sphingolipid, delta(4)-desaturase 1.

However, we observed that natively formed 1-deoxySO showed a different RPLC retention time than a synthetic SPH m18:1(4E)(3OH) standard, though the m/z was identical for both compounds. This suggested that native 1-deoxySO and the synthetic SPH m18:1(4E)(3OH) are structural isomers, probably differing in position and/or configuration of the carbon-carbon double bond. To further elucidate this difference, we used a set of tandem MS methods in combination with total synthesis to elucidate the real double bond position and configuration of native 1-deoxySO.

MATERIALS AND METHODS

Unless stated differently, all solvents and reagents were purchased from Sigma-Aldrich Chemie GmbH (Buchs, Switzerland) excluding methanol, which was purchased from Honeywell Specialty Chemicals Seelze GmBH, Germany.

Cell extract

HEK293 cells were fed with 1 μM deuterium-labeled D_3-1-deoxySA (Avanti Polar Lipids, Alabaster, AL) or with the unlabeled 1-deoxySA (Avanti Polar Lipids). Cells were harvested after 24 h and the whole sphingolipid extract was hydrolyzed to get the free sphingoid bases, as described previously with some modifications (7, 8). The cell pellet was dissolved in 100 μl of PBS. Methanol (500 μl), including D_7-sphingosine and D_7-sphinganine (Avanti Polar Lipids) as the internal standards, was added. Lipids were extracted for 1 h under constant agitation at 37°C. Samples were centrifuged to pellet precipitated proteins and the supernatant was transferred into a new tube. Lipids were hydrolyzed by adding 75 μl of methanolic HCl (1 N HCl and 10 M water in methanol) and incubated for 16 h at 65°C. HCl was neutralized by adding 100 μl of KOH (10 M). Then, 625 μl chloroform was added followed by 100 μl 2 N ammonium hydroxide and 0.5 ml alkaline water to complete phase separation. The sample was vortexed, centrifuged at 16,000 g for 5 min, the upper phase discarded

and the lower (organic) phase washed three times with alkaline water. The organic phase was finally dried under N_2 and stored at −20°C until analysis.

Throughout this work, we refer to the extracted 1-deoxySO as native.

LC-MS method

A commercial 1-deoxySO standard [SPH m18:1(4E)(3OH)] was purchased from Avanti Polar Lipids. SPH m18:1(14Z)(3OH) was synthesized according to the method described below. The SPH m18:1(E)(3OH) standards (5E, 8E, 12E, 13E, and 14E) were synthesized based on an unpublished method that will be issued elsewhere. An LC-MS method described previously (8) was used to compare retention times and in-source fragmentation. Sphingoid bases were separated by RPLC on a C18-column (Uptisphere 120 Å, 5 μm, 125 × 2 mm; Interchim, Montluçon, France) and analyzed on a TSQ Quantum Ultra or a Q Exactive (Thermo, Reinach BL, Switzerland) using an atmospheric pressure chemical ionization (APCI) interface. Mobile phases consisted of ultra-pure water/methanol (1/1 v/v) with 2.6 mM ammonium acetate (mobile phase A) and methanol (mobile phase B). Gradient was set from 50% B to 100% B within 25 min followed by 5 min 100% B and 5 min of equilibration with a flow rate of 0.3 ml/min. For mass spectral detection, the following parameters were set on the APCI source: discharge current of 4 μA, vaporizer temperature of 450°C, sheath gas pressure of 20 AU, auxiliary gas pressure of 5 AU, and capillary temperature of 200°C.

Dimethyl disulfide adduct analysis

Dimethyl disulfide (DMDS, 100 μl) and 20 μl of I_2 (in diethyl ether, 60 mg/ml) were added to whole cell extracts or 15 nmol SPH m18:1(4E)(3OH) standard. Samples were agitated for 16 h in an Eppendorf Thermo shaker at 1,400 rpm and 35°C. The reaction was quenched with 100 μl of 5% aqueous $Na_2S_2O_3$, extracted with 200 μl of hexane, and dried under N_2. Samples were dissolved in 200 μl isopropanol for further analysis according to the method of Dunkelblum, Tan, and Silk (9). The sample was directly injected into the mass spectrometer at a flowrate of 10 μl/min. The [M+H]$^+$ ion of the DMDS adduct of 1-deoxySO was generated by ESI on a Thermo Fisher Scientific Q-Exactive and both collision-induced dissociation (CID) and high-resolution accurate mass analysis were performed. For detection, the following parameters were set on the ESI source: spray voltage of 4.2 kV, vaporizer temperature of 30°C, sheath gas pressure of 5 AU, auxiliary gas pressure 0 AU, capillary temperature of 320°C, and, for fragmentation, in-source CID was performed at 30 eV and higher-energy CID of the ion at m/z 378.3 was performed with a setting of 25.

Differential-mobility spectrometry combined with ozone-induced dissociation

A SelexION^{TM} differential-mobility spectrometer was employed with a QTRAP$^®$5500 triple quadrupole ion-trap mass spectrometer (SCIEX, Ontario, Canada). The instrument was modified for ozone-induced dissociation (OzID) as previously described (10). Solutions for analysis were prepared in LC-grade methanol (VWR Scientific, Murrarie, QLD, Australia) with 5 mM UPLC-grade ammonium acetate (Sigma-Aldrich, St. Louis, MO); SPH standard concentrations were 0.05 μM. Sample solutions were subjected to ESI in a TurboV^{TM} (SCIEX) and passed through the mobility spectrometer. Compensation voltage (CV) applied across the electrodes was scanned while the separation voltage was held constant at 4,100 V. Ionograms were obtained from scanning CV and represent the sum of five mass spectra at each voltage point and have been smoothed using PeakView$^®$ (SCIEX). The ESI source

and differential-mobility spectrometer cell temperatures were 100 and 150°C, respectively; the ESI voltage was set to 5,500 V. Nitrogen was set to 20 psi for each of the following: resolving gas in the differential-mobility spectrometer cell, the nebulizing ESI gas, and the MS curtain gas. Ions exiting the differential-mobility spectrometer cell into the mass spectrometer were mass selected in first quadrupole prior to isolation in the collision cell with ozone present. Ozone was produced by an external generator (Titan; Absolute Ozone, Alberta, Canada) operating at 220 g/Nm^3 (10.3% v/v ozone in oxygen) from which a small portion was mixed into the nitrogen collision gas input to the mass spectrometer through a variable leak valve (Nenion, Lustenau, Austria). The isolation time for ionized lipids in the collision cell was optimized between 100 ms and 15 s depending on the ozone-reactivity of a given ionized lipid (11, 12). Following ozonolysis, ions were transferred to the third quadrupole region where mass analysis was performed using a trap-scan at 1,000 Th/s. OzID spectra obtained at discrete CV values were averaged between 2 and 5 min.

Synthesis of 1-deoxySO [SPH m18:1(14Z)(3OH) or (2S,3R,14Z)-2-aminooctadec-14-en-3-ol]

Eleven intermediate compounds en route to the target SPH m18:1 (14Z)(3OH) were synthesized as described in the supplementary information. A stirred solution of compound **11** (57 mg, 3 mmol) in 1,4-dioxane (1 ml) at 0°C was treated with a solution of 4 M HCl-dioxane (2 ml) over a period of 10 min. The resulting reaction mixture was allowed to stir for 1 h at the same conditions, gradually warmed to ambient temperature, and followed by TLC analysis. After being stirred for an additional 2 h [as monitored by TLC, petroleum ether/EtOAc 4:1, R$_{f(adduct)}$ = 0.5; R$_{f(product)}$ = 0.0; visualized with KMnO$_4$ solution], the reaction mixture was concentrated under reduced pressure. The resultant residue was dissolved in CH$_2$Cl$_2$ (50 ml) and sequentially washed with saturated NaHCO$_3$ solution (40 ml), water (30 ml), and brine solution (40 ml). The organic layer was subsequently dried over anhydrous Na$_2$SO$_4$, filtered, and concentrated in vacuo to afford a pale yellow oily residue. Flash column chromatography of the obtained crude amine over silica gel using ethyl acetate and isopropanol as eluents (from 0 to 10% isopropanol in ethyl acetate) provided the final compound **12** as colorless oil. Yield: 32 mg (71%). R$_f$: 0.32 (EtOAc/isopropanol 4:1, visualized with 1.3% ninhydrin). ^{1}H NMR (500 MHz, MeOD) δ 5.35 (ddd, J = 5.9, 3.6, 2.8 Hz, 2H), 3.70 (ddd, J = 8.1, 5.3, 3.0 Hz, 1H), 3.26 (qd, J = 6.7, 3.1 Hz, 1H), 2.07 – 1.98 (m, 4H), 1.52 (dt, J = 10.3, 8.2 Hz, 1H), 1.47 – 1.41 (m, 2H), 1.41 – 1.28 (m, 18H), 1.21 (d, J = 6.8 Hz, 3H), 0.91 (t, J = 7.4 Hz, 3H). ^{13}C NMR (126 MHz, MeOD) δ 131.05, 130.65, 71.71, 52.61, 34.02, 30.86, 30.75, 30.73, 30.69, 30.65, 30.35, 30.31, 28.15, 27.00, 23.98, 14.16, 12.08. high-resolution MS (ESI$^+$) m/z calculated for C$_{18}$H$_{38}$NO [M+H]$^+$ 284.2953; found 284.2959.

RESULTS

1-deoxySO is a downstream metabolite of 1-deoxySA

HEK293 cells were cultured in the presence of deuterium-labeled D$_3$-1-deoxySA or unlabeled 1-deoxySA. Cells were harvested after 24 h and the profile of the extracted sphingoid bases analyzed by RPLC-MS. We observed the appearance of [M+H]$^+$ ions with m/z 284.3 (unlabeled 1-deoxySO) and of m/z 287.3 (labeled D$_3$-1-deoxySO), which both eluted at the same time from the LC column (**Fig. 1A**), indicating that 1-deoxySO is a product formed downstream of 1-deoxySA (labeled and unlabeled).

Comparison of synthetic SPH m18:1(4E) and native 1-deoxySO

Retention time and APCI in-source fragmentation was compared between native 1-deoxySO and a commercially available synthetic SPH m18:1(4E)(3OH) standard. The native 1-deoxySO eluted from the C18 column after 12.7 min; whereas, the synthetic SPH m18:1(4E)(3OH) eluted after 14.77 min (Fig. 1A). The [M+H]$^+$ ions formed by APCI showed in-source fragmentation and a significant water loss for the SPH m18:1(4E)(3OH) standard, which was considerably less pronounced for the native 1-deoxySO (Fig. 1B). As both molecules showed identical m/z using high-resolution accurate MS (<2 ppm for [M+H]$^+$ and [M+H-H$_2$O]$^+$), the observed deviations in retention time and in-source fragmentation suggested that native 1-deoxySO and the synthetic SPH m18:1(4E)(3OH) were structural isomers.

DMDS derivatization

As the synthetic SPH m18:1(4E)(3OH) and the native 1-deoxySO showed different RPLC properties, we aimed to elucidate the carbon-carbon double bond position of native 1-deoxySO by derivatization with DMDS. The DMDS adducts of 1-deoxySO were analyzed by high-resolution accurate MS using direct injection and ESI. The [M+H]$^+$ ions from the DMDS adducts of 1-deoxySO were selected at m/z 378.3 and subjected to CID. The CID spectrum showed four abundant, but nonspecific, product ions at m/z 330.3 [M+H-CH$_3$SH]$^+$, m/z 312.3 [M+H-CH$_3$SH-H$_2$O]$^+$, m/z 282.3 [M+H-2CH$_3$SH]$^+$, and m/z 264.3 [M+H-2CH$_3$SH-2H$_2$O]$^+$ corresponding to the neutral loss of methane thiols and water as indicated (**Fig. 2**).

Importantly, two less abundant, but structurally diagnostic, product ions were observed at m/z 274.2 (A) and m/z 103.1 (B). These product ions were formed by a cleavage of the carbon-carbon bond between the two methyl sulfide moieties. The mass distribution of the two fragments indicated a double bond in (Δ14)-position for native 1-deoxySO. Product ions indicating a fragmentation at the (Δ4)-position (m/z 243.2 and 134.1) were not detected.

Differential-mobility spectrometry combined with OzID

DMS has previously been deployed successfully for lipid isomer separation prior to mass spectrometric analysis (10, 13). Here it was combined with OzID, which exploits the reaction between mass-selected lipid ions and gaseous ozone inside a mass spectrometer to drive fragmentation diagnostic of the position(s) of carbon-carbon double bonds (12, 14). In these experiments, the D$_3$-labeled hydrolyzed extract from HEK cells was spiked with a 1:1 mixture of the unlabeled commercial SPH m18:1(4E)(3OH) and synthesized SPH m18:1(14E)(3OH) structural isomers and the mixture subjected to ESI. **Figure 3A** shows DMDS ionograms obtained for m/z 284 (black trace) and m/z 287 (red trace) corresponding in mass to the [M+H]$^+$ ions expected from unlabeled and labeled 1-deoxySO, respectively. The black trace shows peaks corresponding to at least two chemically distinction populations of m/z 284
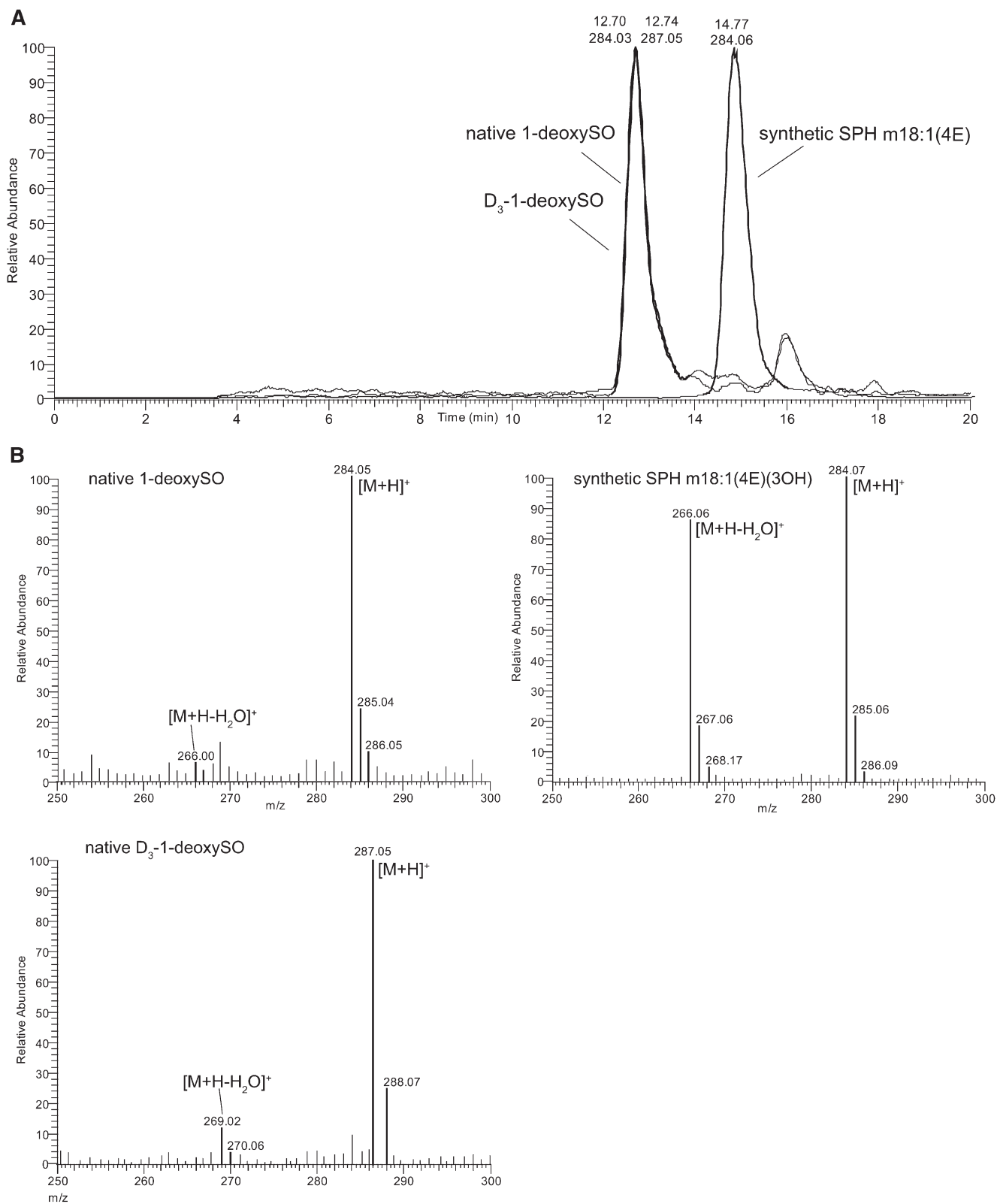
Fig. 1. A: Difference in RPLC retention time of synthetic SPH m18:1(4*E*)(3OH) and native 1-deoxySO extracted from HEK293 cells treated with 1-deoxySA or D$_3$-1-deoxySA. B: APCI in-source fragmentation of a synthetic SPH m18:1(4*E*)(3OH) standard, native 1-deoxySO, and D$_3$-1-deoxySO: the precursor [M+H]$^+$ ion (*m/z* 284) is identical for SPH m18:1(4E)(3OH) and native 1-deoxySO. However, synthetic SPH m18:1(4*E*)(3OH) formed an abundant [M+H-H$_2$O]$^+$ product ion (*m/z* 266), which was formed much less from native 1-deoxySO and D$_3$-1-deoxySO at identical conditions. MS spectra were recorded on a triple quadrupole MS (TSQ Quantum Ultra) with APCI ionization.
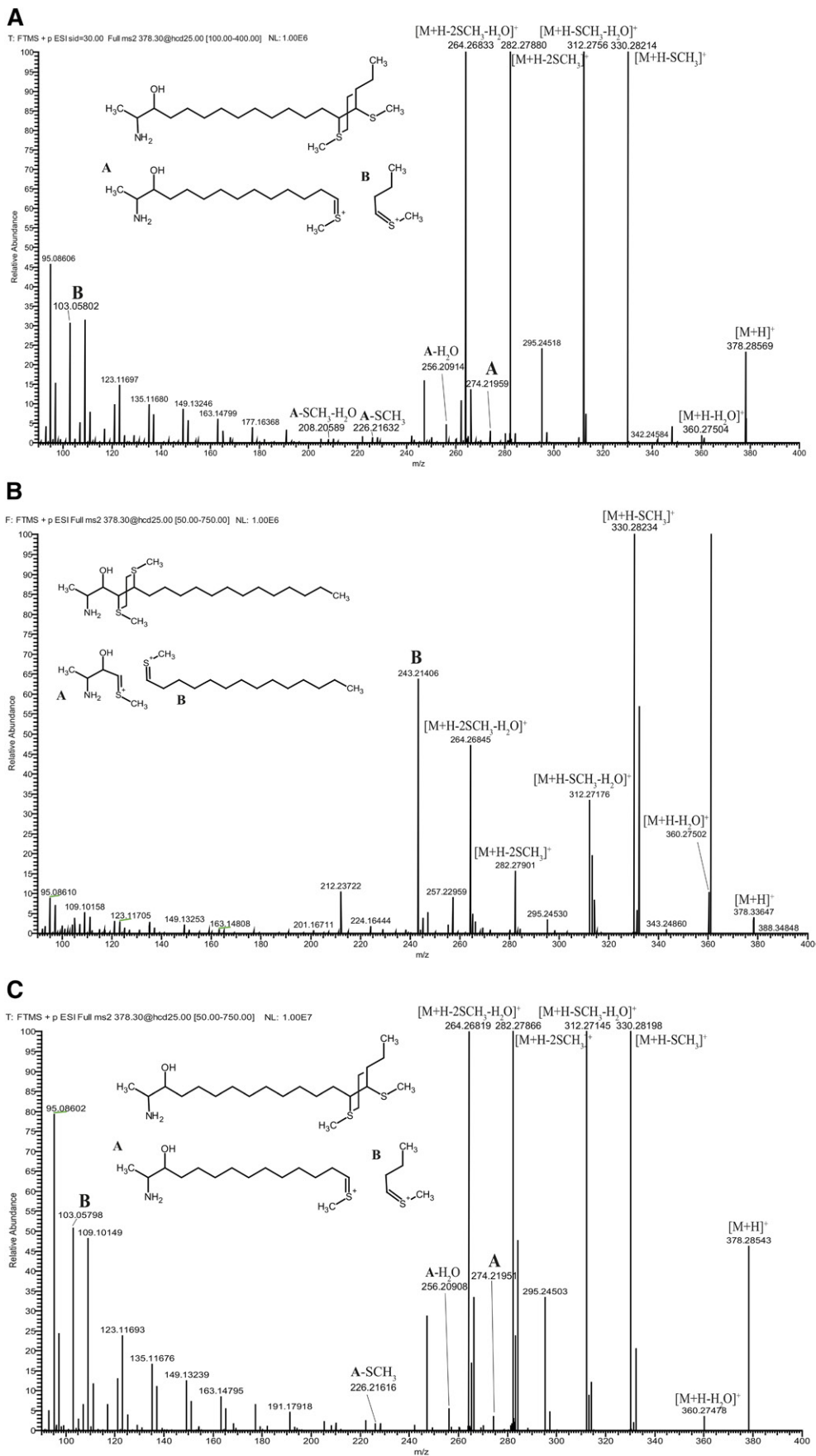
Fig. 2. A: Hydrolyzed lipid extract from HEK293 cells was subjected to DMDS derivatization and analyzed on a high-resolution accurate mass spectrometer using ESI and direct injection. The [M+H]$^+$ ion formed

(i.e., isobars): one with a maximum CV at around 17 V and another peaking at 20 V. Isobars carrying m/z 284 in this mixture should be dominated by the protonated forms of the synthetic SPH m18:1(4E)(3OH) and SPH m18:1(14E) (3OH) isomers. The red trace, corresponding to isobars of m/z 287 (Fig. 3A), showed an analogous pair of peaks at CV 17 and 20 V. These signals could be assigned to [M+H]$^+$ ions arising from native forms of 1-deoxySO present in the cell extract. To interrogate the structure of the ions responsible for each of the two peaks in the ionogram, OzID spectra were acquired for m/z 284 and 287 ions using fixed CV settings of 17 and 20 V. Figure 3B shows product ions arising from the synthetic lipids (at m/z 284) in black and the corresponding D$_3$-labeled native lipid (at m/z 287) in red. Both spectra revealed product ions arising from neutral loss of 40 and 24 Da, characteristic of ozonolysis of a carbon-carbon double bond at the (Δ14)-position on the sphingoid backbone (15) (see supplementary Fig. 1A and supplementary Table 1). Conversely, in the OzID spectra obtained at a CV of 20 V (Fig. 3C), these product ions were absent, while fragments arising from oxidative cleavage of a (Δ4)-double bond (neutral losses of 180 and 164) were observed at m/z 104 and 120 for the unlabeled standard (see supplementary Fig. 1B and supplementary Table 1). Of this pair of ions, the aldehyde is mass-shifted and appears, as expected, at m/z 107 for the D$_3$-isotopologue, while the m/z 123 is absent in this spectrum, possibly due to the lower abundance of the CV = 20 V feature in the native extract. Interestingly, an abundant water loss was observed in the spectra in Fig. 3C, which is much diminished in the spectra in Fig. 3B, providing further evidence of the structural difference between the two lipids.

DMS-OzID analysis was also performed on nonhydrolyzed lipid extract from HEK cells. Four 1-deoxyceramide species could be detected as [M+H]$^+$ ions, consistent with the assignments: Cer m18:1/16:0, Cer m18:1/18:0, Cer m18:1/22:0, and Cer m18:1/24:1. As before, the OzID spectra showed a neutral loss of 40 Da as a characteristic signature for 1-deoxySO with a carbon-carbon double bond at the (Δ14)-position (**Fig. 4**). These data support the presence of the (Δ14) carbon-carbon double bond in both 1-deoxyceramide and the 1-deoxySO and exclude the possibility that the observed (Δ14) desaturation is formed as an artifact of the hydrolysis reaction.

Synthesis of deoxySO standards

Although the previous analysis confirmed the (Δ14) carbon-carbon double bond in native 1-deoxySO, it did not unambiguously assign the stereochemistry of the bond. To further confirm the position and configuration of the double bond, a number of 1-deoxySO analogs with different double bond positions and confirmations (5E,

8E, 12E, 13E, 14E, and 14Z) were synthesized. Here we focus on the synthesis of the SPH m18:1(14Z)(3OH), as details on the synthesis of the other derivatives will be published elsewhere. The synthesis of SPH m18:1(14Z)(3OH) **12** commenced from commercially available 1,10-decanediol (**Scheme 1**). Treatment of 1,10-decanediol with dihydropyran in the presence of a catalytic amount of p-toluenesulfonic acid afforded the mono-THP ether **3** in moderate yield. Subsequent conversion of mono-hydroxyl compound **3** to the corresponding bromo derivative **4** was accomplished through treatment of **3** with tetrabromomethane (CBr$_4$) and triphenyl phosphine (PPh$_3$) to provide compound **4**. With intermediate **4** in hand, the coupling with lithiated 1-pentyne was performed following a previously described protocol (16) with some modifications (see supplementary Table 1 for details). Thus, tert-butyllithium was added to 1-pentyne at $-78°$C, and the in situ generated 1-lithio-1-pentyne was sequentially reacted with DMPU and bromo substrate **4** to afford compound **5** in a satisfactory yield. Subsequent stereoselective hydrogenation of alkyne **5** was accomplished with Lindlar catalyst after optimization of reaction conditions to afford the desired Z-configuration of the alkene **6** as a sole isomer (see supplementary Table 2 for more details). It is noteworthy that initial attempts to furnish alkene **6** led to a product that was contaminated (10–15%) with inseparable by-products. Careful analysis of ^{1}H-NMR spectra of the crude mixture identified these by-products as the E-configured alkene and the over-reduced product, 1-bromopentadecane. Cleavage of the THP-protecting group in **6** under acid-catalyzed ethanol treatment proceeded smoothly to provide the hydroxyl alkene **7**, which was subsequently subjected to Appel reaction with CBr$_4$/PPh$_3$ to furnish the Z-bromo-alkene **8**.

Next, the obtained bromo-alkenyl chain **8** was converted into the corresponding Grignard reagent **9** and subsequently coupled to the Weinreb amide **2** (prepared from L-alanine in two steps, see the supplementary information for details). Toward this end, Weinreb amide **2** was reacted with 0.9 equivalent of methylmagnesium bromide (as sacrificial base), followed by addition of the Grignard reagent **9** to afford ketone **10** in 78% isolated yield. The subsequent diastereoselective reduction of the carbonyl group in **10** with lithium tri-(tert-butoxy)-aluminum hydride (1.7 equivalent) in absolute ethanol at $-78°$C was accomplished without reduction of the double bond to furnish the desired anti-amino alcohol **11** as a mere stereoisomer. Acidic hydrolysis of the tert-butyl carbamate protecting group of **11** with 4 M HCl-dioxane solution yielded the corresponding hydrochloric salt of SPH m18:1(14Z)(3OH) (.HCl). The desired product **12** was finally obtained after neutralization workup in 71% yield.

from DMDS adduct of native 1-deoxySO (m/z of 378.2857) was in excellent agreement (<1 ppm) with the calculated m/z of 378.2859 (C$_{20}$H$_{44}$NOS$_2^+$). The precursor ion was selected for CID yielding to the spectrum shown. Product ions A (m/z 274) and B (m/z 103) are indicated in the spectrum and are diagnostic for a fragmentation at (Δ14) position. B: Spectrum from SPH m18:1(4E)(3OH) showing product ion B (m/z 243). C: Spectrum from SPH m18:1(14Z)(3OH) showing product ions A (m/z 274) and B (m/z 103). Putative structures for the diagnostic product ions are shown as insets in the spectra.
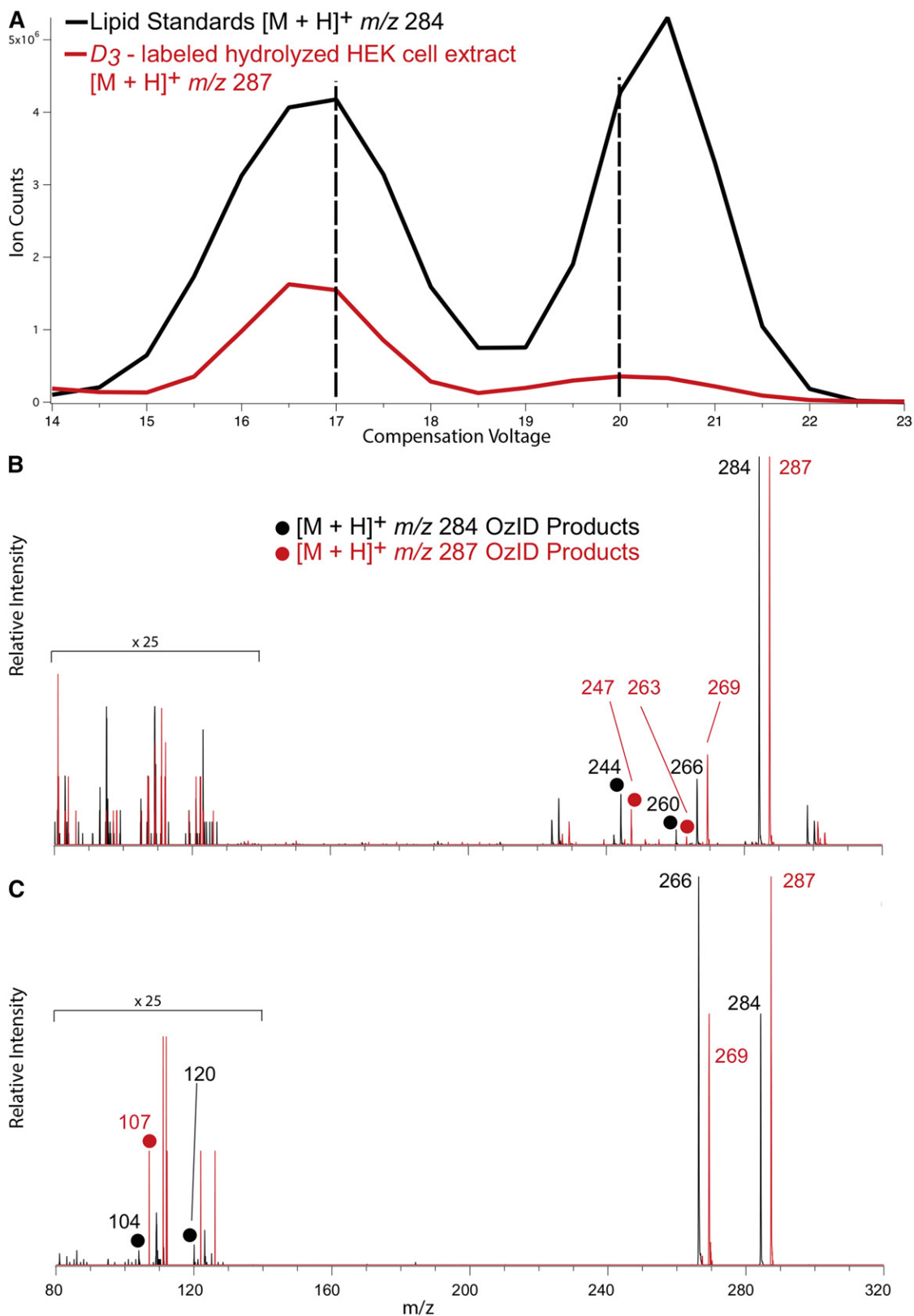
Fig. 3. ESI(+) was undertaken on a mixture of D₃-labeled hydrolyzed HEK cell lipid extracts spiked with unlabeled synthetic standards, SPH m18:1(4E)(3OH) and SPH m18:1(14E)(3OH). A: Ionograms showing separation in voltage space of the [M+H]⁺ ions formed from the two lipid isomers. Each of the synthetic lipids spiked into the extract produced a peak in the black trace (*m/z* 284) and similar features were observed for the labeled HEK293 extract shown in the red trace (*m/z* 287). B: OzID spectra obtained for synthetic standard (black spectrum) and the D₃-labeled extract (red spectrum) corresponding to the first feature in the ionogram (i.e., CV = 17 V ozone reaction time of 100 ms). C: OzID spectra obtained for synthetic standard (black spectrum) and the D₃-labeled extract (red spectrum) corresponding to the second feature in the ionogram (i.e., CV = 20 V ozone reaction time of 15 s). OzID product ions characteristic of the locations of the carbon-carbon double bonds are indicated by closed circles and enable assignment of the position of unsaturation to (Δ14)-position (B) and (Δ4)-position (C).
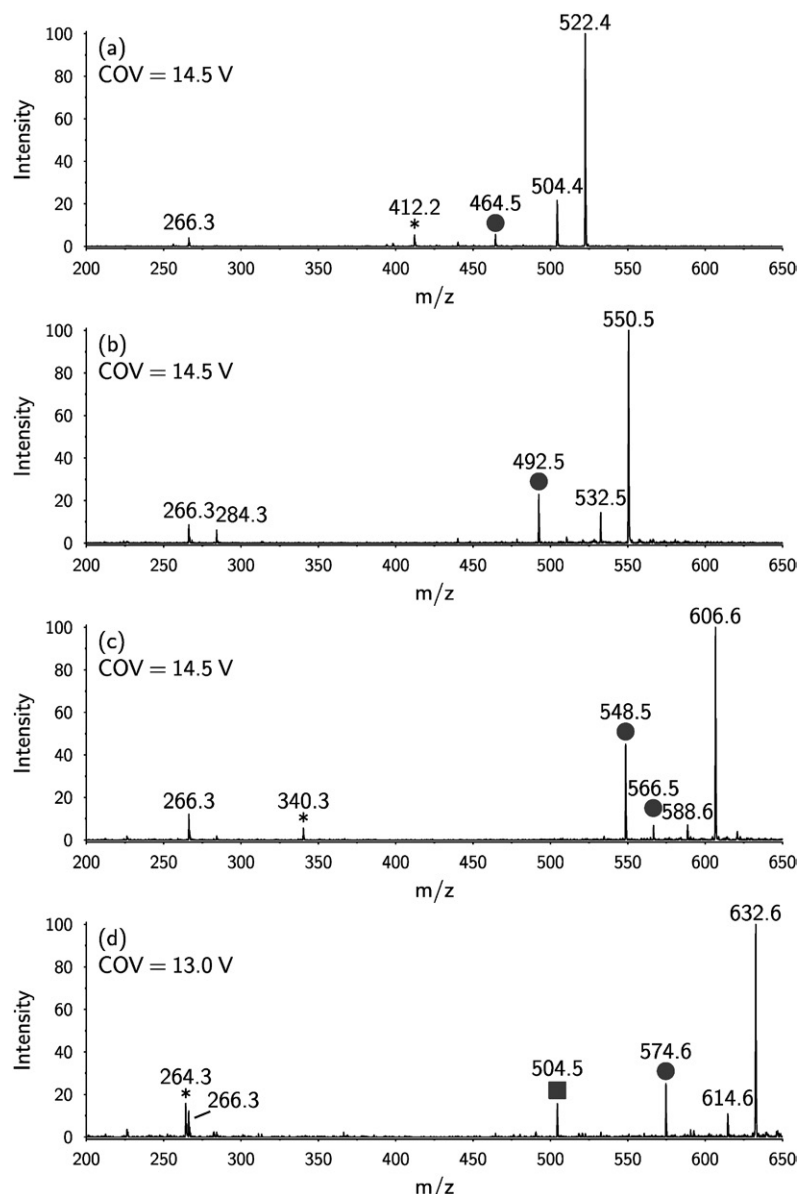
Fig. 4. ESI(+)-OzID spectra obtained for *m/z* values corresponding to deoxyceramides present in an non-hydrolyzed HEK cell lipid extract. All spectra show a product ion at *m/z* 266, which is consistent with the collision-induced dehydration of the backbone followed by cleavage of the amide bond to liberate the acyl chain. Product ions arising from a characteristic neutral loss of 40 Da from the $[M+H]^+$ or $[M+H-H_2O]^+$ are marked with circles and are consistent with an n-4 double bond (i.e., a $\Delta 14$ double bond in the SPH m18:1 backbone). Product ions arising from a characteristic neutral loss of 110 Da from the $[M+H]^+$ or $[M+H-H_2O]^+$ are marked with squares and are consistent with the presence of an n-9 double bond (e.g., 24:1 $\Delta 15$ acyl chain). These spectra are consistent with the deoxyceramides Cer m18:1($\Delta 14$)/16:0 (A), Cer m18:1($\Delta 14$)/18:0 (B), Cer m18:1($\Delta 14$)/22:0 (C), and Cer m18:1($\Delta 14$)/24:1($\Delta 15$) (D) (see also supplementary Fig. 2 and supplementary Table 1). Product ions marked with an asterisk (*) showed different mobility characteristics to the OzID peaks and likely arise from isobaric interference.

Retention-time correlation of native lipids with synthetic standards

The RPLC retention times of the synthetic SPH m18:1(*E*)(3OH) standards with double bonds in positions 5*E*, 8*E*, 12*E*, and14*E* were compared. We observed an inverse logarithmic correlation ($R^2 = 0.96$) between retention times and the double bond position (**Fig. 5A**). The more the double bond (DB) was positioned toward the omega end, the earlier the molecule eluted from the column. The closest match in retention time between native 1-deoxySO and the synthetic standards was seen again for SPH m18:1(14*E*)(3OH), although the elution time between the two compounds still differed by about 30 s (Fig. 5B).

To further elucidate the DB configuration, we compared the retention times of native 1-deoxySO with the synthetic standard in (14*Z*) configuration (Fig. 5B, supplementary Fig. 3). The SPH m18:1(14*Z*) eluted at 13.0 min and therefore coincided with the elution time of native 1-deoxySO.

From these results, we conclude that native 1-deoxySO bears a (14*Z*) double bond.

DISCUSSION

The 1-deoxySO is an atypical sphingolipid that lacks the 1-hydroxyl group of canonical sphingosine. It is a downstream metabolite of 1-deoxySA, which is formed by SPT due to its alternative activity with alanine. Because of the missing C1-hydroxyl group, 1-deoxySO cannot be phosphorylated to S1P and, therefore, also cannot be degraded by S1P-lyase (2).

Pathologically elevated 1-deoxySLs play an important role in the inherited neuropathy HSAN I but were also found in other conditions, like the metabolic syndrome and type 2 diabetes (3, 7). However, the metabolism of 1-deoxySLs and their molecular structures have not been investigated in detail yet. Comparing native 1-deoxySO to
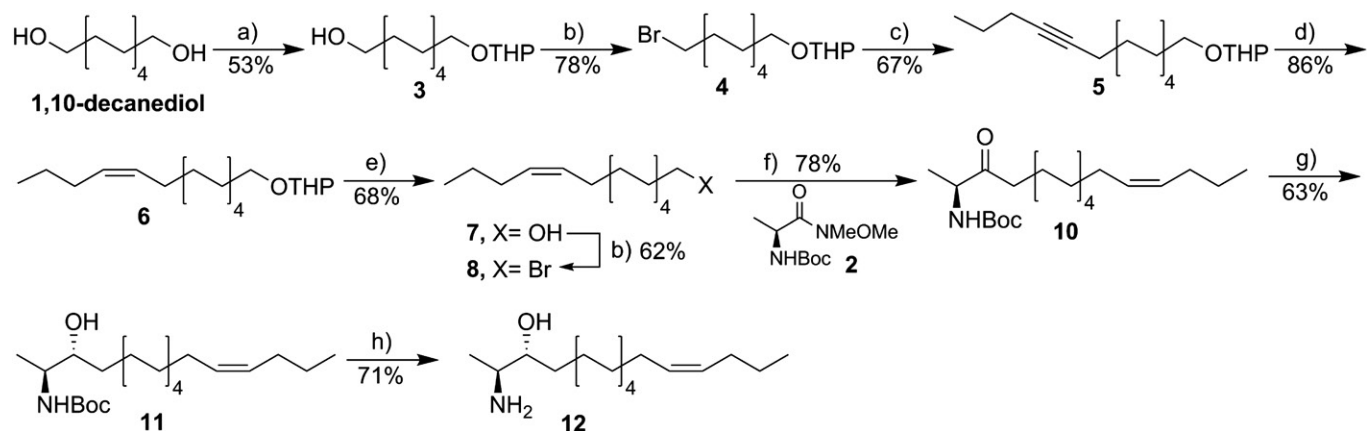
Scheme 1. Synthesis of the 14*Z*-deoxySO analog. Reagents and conditions: DHP, *p*-toluenesulfonic acid (cat.), THF:DCM, 0°C-rt, 12 h (a); CBr$_4$, PPh$_3$, DCM, 0°C-rt, 4 h (b); *i*) 1-pentyne, *tert*-BuLi, toluene, −78°C, 1 h, and then *ii*) DMPU, 4, THF, −78°C-rt, 7 h (c); H$_2$, EDA, Lindlar catalyst, 5% DMF in EtOAc, 0°C, 6 h (d); PPTS (cat.), ethanol, 62°C, 2 h (e); *i*) Mg, 1,2-DBE (drops), Et$_2$O, reflux, 2 h, and then *ii*) 2, MeMgBr, DCM:Et$_2$O, reflux, 2 h (f); tri-(*tert*-butoxy)-aluminum hydride, ethanol, −78°C, 1 h (g); 4 M HCl-dioxane, 0°C, 3 h (h).

a synthetic SPH m18:1(4*E*) standard by RPLC, we observed a significant deviation in retention time, although the *m/z* was identical for both molecules. Analyzing the DMDS derivatized adducts of native 1-deoxySO by MS^2 revealed two specific fragments, which indicated the double bond position at (Δ14) and, therefore, distinct to that of the canonical (Δ4)-position. The (Δ14)-position was further confirmed using differential-mobility spectrometry combined with OzID. Comparing retention times of native 1-deoxySO to a set of synthetic SPH m18:1 standards finally confirmed a (14*Z*) DB in native 1-deoxySO.

During sphingolipid de novo synthesis, the sphingolipid delta(4)-desaturase 1 normally introduces a (4*E*) double bond into the sphingoid base backbone of dihydroceramide to form ceramide. The observation that native

1-deoxySO bears a (14*Z*) instead of a (4*E*) DB indicates that the metabolism of 1-deoxySL deviates from that of canonical sphingolipids. Interestingly, sphingadiene, a polyunsaturated downstream product of sphingosine (17), has double bonds at both the (4*E*) and (14*Z*) positions (Fig. 5C). The presence of a (14*Z*) double bond in both sphingadiene and native 1-deoxySO suggests that both metabolites are substrates of the same desaturase, although the responsible enzyme is unknown so far (18). The fact that exogenously added D$_3$-lableled 1-deoxySA is converted to D$_3$-labeled 1-deoxySO also showed that the double bond is introduced downstream of 1-deoxySA and not formed by an SPT-mediated incorporation of an unsaturated acyl-CoA. Interestingly, 1-deoxymethylsphingosine, the corresponding downstream product of 1-deoxymethylsphinganine,
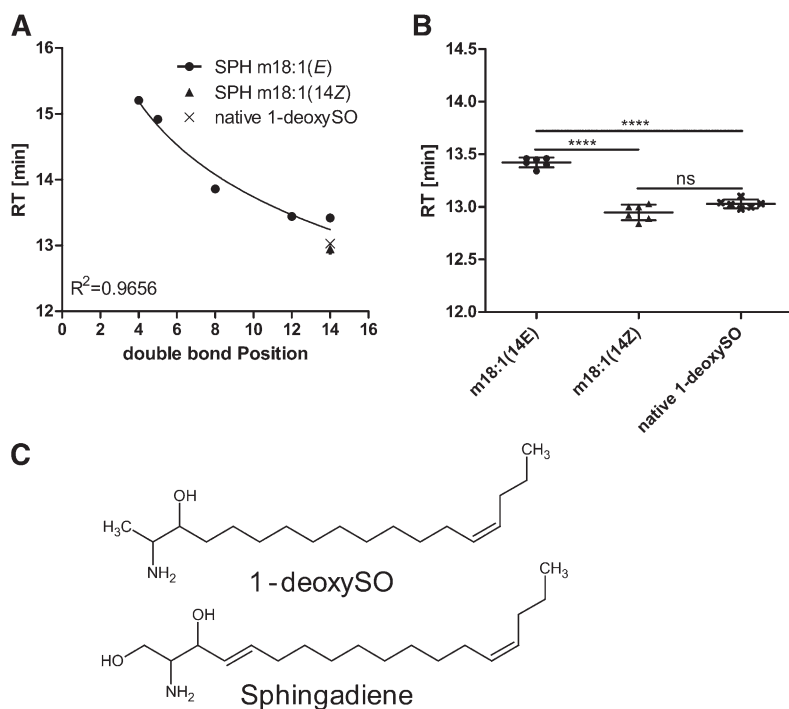

Fig. 5. A: RPLC retention times (RT) for a set of synthetic SPH m18:1 standards having double bonds in positions (4*E*), (5*E*), (8*E*), (12*E*), and (14*E*). The position of the double bond within the alkyl chain showed a logarithmic correlation to the retention times. B: Comparing the retention times of native 1-deoxySO to the synthetic standards, SPH m18:1 (14*Z*) and SPH m18:1 (14*E*), identified native 1-deoxySO as SPH m18:1 (14*Z*) (****P< 0.0001). C: Comparison of the chemical structures of 1-deoxySO and sphingadiene.

which is formed by the condensation with glycine, seems to contain a (3*E*) DB. The *m/z* as well as RPLC retention time of native 1-deoxymethylsphingosine matched that of a synthetic m17:1 (3*E*)(2OH) standard (supplementary Fig. 4). As 1-deoxymethylsphingosine contains only 17 carbons, this equals the (4*E*) DB position of canonical sphingolipids.

In conclusion we provide strong evidence from multiple orthogonal analytical techniques to unambiguously assign native 1-deoxySO as it is formed in HEK293 cells to be a SPH m18:1(14*Z*)(3OH) structure. This furthermore implies that 1-deoxyceramides are metabolized distinct from canonical sphingolipids. However, more detailed studies are needed to further investigate the enzymatic pathways and metabolic steps involved in the conversion of these lipids.▮

Note added in proof

The second author name, Essa M. Saied, appeared as Essa Mostafa in the PiP version of the article and has been changed in the final version at the request of the authors.

REFERENCES

1. Merrill, A. H., Jr. 2011. Sphingolipid and glycosphingolipid metabolic pathways in the era of sphingolipidomics. *Chem. Rev.* **111:** 6387–6422.
2. Zitomer, N. C., T. Mitchell, K. A. Voss, G. S. Bondy, S. T. Pruett, E. C. Garnier-Amblard, L. S. Liebeskind, H. Park, E. Wang, M. C. Sullards, et al. 2009. Ceramide synthase inhibition by fumonisin B1 causes accumulation of 1-deoxysphinganine: a novel category of bioactive 1-deoxysphingoid bases and 1-deoxydihydroceramides biosynthesized by mammalian cell lines and animals. *J. Biol. Chem.* **284:** 4786–4795.
3. Penno, A., M. M. Reilly, H. Houlden, M. Laura, K. Rentsch, V. Niederkofler, E. T. Stoeckli, G. Nicholson, F. Eichler, R. H. Brown, Jr., et al. 2010. Hereditary sensory neuropathy type 1 is caused by the accumulation of two neurotoxic sphingolipids. *J. Biol. Chem.* **285:** 11178–11187.
4. Jun, B. K., A. Chandra, D. Kuljis, B. P. Schmidt, and F. S. Eichler. 2015. Substrate availability of mutant SPT alters neuronal branching and growth cone dynamics in dorsal root ganglia. *J. Neurosci.* **35:** 13713–13719.
5. Zuellig, R. A., T. Hornemann, A. Othman, A. B. Hehl, H. Bode, T. Guntert, O. O. Ogunshola, E. Saponara, K. Grabliauskaite, J. H. Jang, et al. 2014. Deoxysphingolipids, novel biomarkers for type 2 diabetes, are cytotoxic for insulin-producing cells. *Diabetes.* **63:** 1326–1339.
6. Othman, A., R. Bianchi, I. Alecu, Y. Wei, C. Porretta-Serapiglia, R. Lombardi, A. Chiorazzi, C. Meregalli, N. Oggioni, G. Cavaletti, et al. 2015. Lowering plasma 1-deoxysphingolipids improves neuropathy in diabetic rats. *Diabetes.* **64:** 1035–1045.
7. Othman, A., M. F. Rütti, D. Ernst, C. H. Saely, P. Rein, H. Drexel, C. Porretta-Serapiglia, G. Lauria, R. Bianchi, A. v. Eckardstein, et al. 2012. Plasma deoxysphingolipids: a novel class of biomarkers for the metabolic syndrome? *Diabetologia.* **55:** 421–431.
8. Othman, A., R. Benghozi, I. Alecu, Y. Wei, E. Niesor, A. von Eckardstein, and T. Hornemann. 2015. Fenofibrate lowers atypical sphingolipids in plasma of dyslipidemic patients: A novel approach for treating diabetic neuropathy? *J. Clin. Lipidol.* **9:** 568–575.
9. Dunkelblum, E., S. H. Tan, and P. J. Silk. 1985. Double-bond location in monounsaturated fatty acids by dimethyl disulfide derivatization and mass spectrometry: Application to analysis of fatty acids in pheromone glands of four lepidoptera. *J. Chem. Ecol.* **11:** 265–277.
10. Maccarone, A. T., J. Duldig, T. W. Mitchell, S. J. Blanksby, E. Duchoslav, and J. L. Campbell. 2014. Characterization of acyl chain position in unsaturated phosphatidylcholines using differential mobility-mass spectrometry. *J. Lipid Res.* **55:** 1668–1677.
11. Pham, H. T., A. T. Maccarone, J. L. Campbell, T. W. Mitchell, and S. J. Blanksby. 2013. Ozone-induced dissociation of conjugated lipids reveals significant reaction rate enhancements and characteristic odd-electron product ions. *J. Am. Soc. Mass Spectrom.* **24:** 286–296.
12. Poad, B. L., H. T. Pham, M. C. Thomas, J. R. Nealon, J. L. Campbell, T. W. Mitchell, and S. J. Blanksby. 2010. Ozone-induced dissociation on a modified tandem linear ion-trap: observations of different reactivity for isomeric lipids. *J. Am. Soc. Mass Spectrom.* **21:** 1989–1999.
13. Shvartsburg, A. A., G. Isaac, N. Leveque, R. D. Smith, and T. O. Metz. 2011. Separation and classification of lipids using differential ion mobility spectrometry. *J. Am. Soc. Mass Spectrom.* **22:** 1146–1155.
14. Thomas, M. C., T. W. Mitchell, D. G. Harman, J. M. Deeley, J. R. Nealon, and S. J. Blanksby. 2008. Ozone-induced dissociation: elucidation of double bond position within mass-selected lipid ions. *Anal. Chem.* **80:** 303–311.
15. Brown, S. H., T. W. Mitchell, and S. J. Blanksby. 2011. Analysis of unsaturated lipids by ozone-induced dissociation. *Biochim. Biophys. Acta.* **1811:** 807–817.
16. Chen, J., Y. Li, and X. P. Cao. 2006. First stereoselective synthesis of serinol-derived malyngamides and their 1′-epi-isomers. *Tetrahedron Asymmetry.* **17:** 933–941.
17. Zhang, T., L. Barclay, L. D. Walensky, and A. Saghatelian. 2015. Regulation of mitochondrial ceramide distribution by members of the BCL-2 family. *J. Lipid Res.* **56:** 1501–1510.
18. Renkonen, O., and E. L. Hirvisalo. 1969. Structure of plasma sphingadienine. *J. Lipid Res.* **10:** 687–693.